Communicated by Dr Hu Jun

Accepted Manuscript

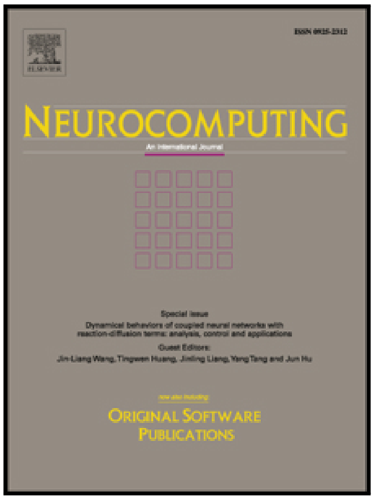

Improved quasi-synchronization criteria for delayed fractional-order memristor-based neural networks via linear feedback control

Yingjie Fan, Xia Huang, Zhen Wang, Yuxia Li

PII: S0925-2312(18)30459-4
DOI: 10.1016/j.neucom.2018.03.060
Reference: NEUCOM 19492

To appear in: *Neurocomputing*

Received date: 20 November 2017
Revised date: 8 March 2018
Accepted date: 26 March 2018

Please cite this article as: Yingjie Fan, Xia Huang, Zhen Wang, Yuxia Li, Improved quasi-synchronization criteria for delayed fractional-order memristor-based neural networks via linear feedback control, *Neurocomputing* (2018), doi: 10.1016/j.neucom.2018.03.060

Improved quasi-synchronization criteria for delayed fractional-order memristor-based neural networks via linear feedback control *

Yingjie Fan[a], †Xia Huang[a], Zhen Wang[b], Yuxia Li[a]
[a] College of Electrical Engineering and Automation,
Shandong University of Science and Technology, Qingdao 266590, China
[b] College of Mathematics and Systems Science,
Shandong University of Science and Technology, Qingdao 266590, China

Abstract: This paper is concerned with the quasi-synchronization of two delayed fractional-order memristor-based neural networks (FMNNs) with mismatched switching jumps via linear feedback control. The concept of asynchronous switching time interval (ASTI) is introduced first to describe when the drive-response FMNNs update their connection weights asynchronously. Under the framework of fractional-order differential inclusions, two improved quasi-synchronization criteria, expressed by algebraic conditions and LMIs conditions respectively, are established by constructing appropriate Lyapunov functionals in combination with some fractional-order differential inequalities. Different from most previously published works, the synchronization error bound can be estimated without requiring the bound of chaotic trajectories. In addition, it has been shown that the degree of mismatch between the switching jumps has an important influence on the distribution of ASTI as well as the practical synchronization error. Finally, two numerical examples are given to verify the validity and feasibility of the obtained results.

Keywords: Quasi-synchronization; Fractional-order; Memristor-based neural networks; Linear feedback control; Switching jumps; Asynchronous switching time interval.

1 Introduction

In recent years, considerable attention has been attracted to fractional-order dynamical systems due to their widespread applications in many fields such as neural systems [1], financial systems [2], and viscoelastic systems [3]. As a generalization of integration and differentiation from integer-order to arbitrary non-integer order, a distinguished feature of fractional-order systems is that they have long-term memory effects, which makes it suitable for describing various materials and processes more precisely [4]. In the field of electronics, the model of fractional capacitor, formally called the fractance, has been presented, which describes the fractional differentiation constitutive relationship $I(t) = C\frac{d^\alpha V(t)}{dt^\alpha} \equiv C\ D_t^\alpha V(t)$ between the voltage $V(t)$ and the current $I(t)$ passing through it [5]-[6]. Neural networks (NNs) have found a wide scope of applications in signal processing, image processing, combinatorial optimization, pattern recognition, and associative memories. In recent years, as an important application area of fractional-order

*This work was supported by the National Natural Science Foundation of China under Grants 61473178, 61573008 61473177.

†Corresponding author (huangxia_qd@126.com)

systems, fractional-order neural networks (FNNs) have been proposed by replacing the common capacitors in circuit implementation of integer-order NNs by fractional capacitors to improve the accuracy of the NNs model. It has been shown that fractional derivatives provide neurons with a fundamental and general computational ability that contributes to efficient information processing [1]. As a hot spot, some remarkable results relating to stability and synchronization of FNNs have been reported in [7]-[12].

Memristors, as the fourth fundamental electrical component along with resistors, inductors and capacitors, were postulated by circuit theorist Leon Chua [13] and realized by Hewlett-Packard research team [14]. This new nonlinear circuit element describes the relationship between the electric charge and magnetic flux. It has been testified that synapses can be implemented with the aid of memristors in order to imitate the functions of brain in analog circuits [15]. As a result, many scholars and researchers replaced resistors in the conventional NNs by memristors and proposed the memristor-based neural networks (MNNs) [16]-[17]. In comparison with NNs, MNNs have more complex dynamical behavior. Up to now, considerable efforts have been devoted to the study of MNNs including stability [18]-[19], stabilization [20]-[21], dissipativity [22], and synchronization [23]-[28]. Furthermore, considering the fractional order characteristics of a real capacitor, fractional-order memristor-based neural networks (FMNNs) can be accordingly established if the common capacitors in circuit implementations of MNNs are substituted with fractional capacitors to improve the accuracy of the MNNs model. But it is worth pointing out that the traditional control methods for MNNs are no longer applicable to FMNNs, since FMNNs are represented by fractional-order differential equations. During these years, more and more researchers have devoted themselves to seeking for effective methods for investigating the dynamics of FMNNs such as stability [29], attractivity [30], and stabilization [31]. For instance, by using some fractional-order differential inequalities techniques, global Mittag-Leffler stability of FMNNs was investigated in [29]. By employing Lyapunov functionals method, the global attractivity of FMNNs was discussed in [30]. Global stabilization of FMNNs was achieved via state feedback control or output feedback control in [31].

Synchronization means an agreement or correlation of different processes in time. In recent years, some researchers have concentrated their effort on synchronization of FMNNs [32]-[36] due to their potential applications in information science and biological systems. In particular, a synchronization criterion for FMNNs with multiple delays was obtained by employing the maximum modulus principle and the spectral radius of matrices in [34]. Considering the effect of parameter uncertainty, synchronization was studied for delayed FMNNs by combining comparison theorem with Lyapunov method in [35]. Lag synchronization for FMNNs was discussed via periodically intermittent control in [36]. However, from a practical viewpoint, parameter mismatches are inevitable in the implementation of synchronization due to limited fabrication techniques and measuring tools. The mismatches between parameters may destroy the synchronization of drive-response systems. It is thus important and also interesting to reconsider the synchronization problem in case of parameter mismatches. Whereas, if the parameter mismatches are relatively small, the synchronization error may be controlled within a small region, which is described as quasi-synchronization. Synchronization of chaotic systems with parameter mismatches has been studied in [37]-[40]. For instance, quasi-synchronization was studied for delayed chaotic systems with parameter mismatches by using intermittent linear feedback control [37]. The optimization problem for quasi-synchronization was investigated for heterogeneous dynamic networks via distributed impulsive control [39]. Besides, some quasi-synchronization criteria were established for FMNNs with mismatched memristive connection weights based on a new estimate of Mittag-Leffler function and a hybrid controller in [40]. But most of the chaotic systems involved in aforementioned works are integer-order except [40].

It is well known that FMNN is essentially a switched nonlinear system owing to the dependence of memristive connection weights on neuronal states, as well as the switching jumps. Then, for drive-response FMNNs, if they differ only in initial values or switching jumps, they would have the chance to stay in different subsystems. It implies that any difference between the initial values or the switching jumps will give rise to undesirable error. The emergence of the undesirable error will bring more difficulties to system analysis and control design. However, it should be pointed out that the synchronization schemes in most previously published works are predominantly concentrated on the synchronization of identical FMNNs and little effort has been given to the synchronization of FMNNs with mismatched switching jumps. Also, most of the synchronization controllers therein are complicated. From the above analysis, we can find that the underlying mechanisms for the influence of mismatched switching jumps on synchronization need to be revealed.

In order to qualitatively investigate the effect of the mismatched switching jumps on synchronization of FMNNs, we introduce the concept of asynchronous switching time interval (ASTI) in this paper. We say that there exists a asynchronous switching time interval (ASTI), if the memristive connection weights of the drive and response systems switch asynchronously. Thus, it is interesting to know: (1) what's the relationship between the switching jumps and the estimated synchronization error; (2) what's the influence of the mismatched switching jumps on ASTI and practical synchronization error? However, to the best of our knowledge, this is still an open problem and therefore deserves further investigation. Hence, we investigate the quasi-synchronization of delayed FMNNs with mismatched switching jumps.

It should be noted that the previously published results regarding stability, stabilization and synchronization of FMNNs are all expressed by algebraic conditions [29]-[36]. Obviously, it is inconvenient to verify such kind of algebraic conditions because one has to check them one by one for n times. As is well known, LMI-based analysis technique has been generally accepted as an effective method to deal with a variety of dynamical systems because the feasible solution of the LMIs conditions can be easily solved by MATLAB LMI toolbox. However, the existing LMI-based analysis techniques developed in [9, 41, 42, 43, 44] are inapplicable to fractional-order nonlinear systems with delay. To fill this gap, two new inequalities about differential inclusions are established to achieve the quasi-synchronization criteria expressed by LMI form. In addition, it should be mentioned that all the previously published results [37]-[40] on quasi-synchronization are obtained under the assumption that the trajectories of chaotic systems are bounded. It means that the bound of the trajectories of the chaotic systems being considered must be known in advance. As is well known, the problem of state estimation is very important and is a major requisite for the design and control of dynamical systems [45]-[49]. However, sometimes it is hard to obtain the information of the real-time states. Besides, notice that the bound of the chaotic trajectories depends on the initial values. It implies that if the initial value varies, the bound has to be evaluated again. To solve this problem, we develop a new method in this paper to achieve some improved quasi-synchronization criteria without the bound of the chaotic trajectories.

Motivated by the aforementioned discussions, the main objective of this paper is to discuss quasi-synchronization of delayed FMNNs with mismatched switching jumps via linear feedback control. The main contributions of this paper are highlighted as follows. First, two new inequalities about differential inclusions are established, which play an important role in the estimation of synchronization error bound. Second, two improved quasi-synchronization criteria, expressed by algebraic conditions and LMIs conditions respectively, are derived by constructing suitable Lyapunov functionals, together with some fractional differential inequalities. Compared with some previously obtained results [37]-[40], the synchronization error bound depends on the switching jumps and the assumption on the boundedness of chaotic systems is dropped. Third, the influence of the degree of mismatch between switching jumps on practical synchronization error and ASTI is discussed for the first time. It has been shown that the ASTI and practical synchronization error depend heavily on the degree of mismatch. The obtained results extend and improve some existing results on FMNNs.

The rest of this paper is organized as follows. In Section 2, some lemmas, definitions and assumptions are introduced and the problem of quasi-synchronization is formulated. In Section 3, the synchronization control schemes for FMNNs are designed and several improved quasi-synchronization criteria are derived. In Section 4, two numerical examples are provided to illustrate the feasibility of the proposed theoretical results. Finally, some conclusions are drawn in Section 5.

2 Preliminaries and Problem Formulation

Notations. Throughout this paper, the notation $||\cdot||_p$ $(p = 1, 2)$ is used to denote the p-norm for a vector or for a matrix. Besides, solutions of all the systems are considered in Filippov's sense. R is the space of real number. R^n denotes the n-dimensional Euclidean space. $R^{n\times n}$ denotes the set of $n \times n$ real matrices. $diag(\nu_1, \nu_2, \dots, \nu_n)$ denotes a diagonal matrix. For matrix $A = (a_{ij})_{n\times n}$, $|A| = (|a_{ij}|)_{n\times n}$. $A < 0$ (respectively, $A > 0$) means that A is symmetric and negative definite (respectively, symmetric and positive definite). $\lambda_{\min}(A)$ stands for the smallest eigenvalue of matrix A. A^T and A^{-1} represent the transpose and the inverse of matrix A, respectively. Let $\tau > 0$, $C([-\tau, 0], R^n)$ denotes the family of continuous functions from $[-\tau, 0]$ to R^n.

2.1 Definitions and lemmas

Definition 1 *[50]. The fractional integral of order α for a function $f(t)$ is defined as*

$$ {}_{t_0}I_t^\alpha f(t) = \frac{1}{\Gamma(\alpha)} \int_{t_0}^{t} (t-\tau)^{\alpha-1} f(\tau) d\tau, $$

where $t \geq t_0$, $\alpha > 0$, and $\Gamma(\cdot)$ is the Gamma function, that is, $\Gamma(\alpha) = \int_0^{+\infty} e^{-t} t^{\alpha-1} dt$.

Definition 2 *[50]. The Caputo fractional derivative of order α for a function $f(t)$ is defined as*

$$ {}_{t_0}D_t^\alpha f(t) = \frac{1}{\Gamma(n-\alpha)} \int_{t_0}^{t} \frac{f^{(n)}(\tau)}{(t-\tau)^{\alpha-n+1}} d\tau, $$

where $t \geq t_0$, and n is the positive integer such that $n-1 < \alpha < n$. In particular, when $0 < \alpha < 1$, we have

$$ {}_{t_0}D_t^\alpha f(t) = \frac{1}{\Gamma(1-\alpha)} \int_{t_0}^{t} (t-\tau)^{-\alpha} f'(\tau) d\tau. $$

Definition 3 *[51]. Suppose $E, Y \subset R^n$, then $F : E \to Y$ is called a set-valued map, if for each point $x \in E$, there corresponds a nonempty set $F(x) \subset Y$. A set-valued map F with nonempty values is said to be upper-semi-continuous at $x_0 \in E \subset R^n$ if, for any open set N containing $F(x_0)$, there exists a neighborhood M of x_0 such that $F(M) \subset N$. $F(x)$ is said to have a closed (convex, compact) image if, for each $x \in E$, $F(x)$ is closed (convex, compact).*

Definition 4 *[52]. Consider the system $\frac{dx}{dt} = g(x)$, $x \in R^n$, with discontinuous right-hand sides, a set-valued map is defined as*

$$ \phi(x) = \bigcap_{\delta>0} \bigcap_{\mu(N)=0} K[g(B(x,\delta)\backslash N)], $$

where $K[E]$ is the closure of the convex hull of set E, $B(x,\delta) = \{y : \|y-x\| \leq \delta\}$, and $\mu(N)$ is the Lebesgue measure of set N. A solution in Filippov's sense of the Cauchy problem for this system with initial condition $x(0) = x_0$ is an absolutely continuous function $x(t)$, $t \in [0,T]$, which satisfies $x(0) = x_0$ and differential inclusion:

$$\frac{dx}{dt} \in \phi(x)$$

for a.e. $t \in [0,T]$.

Lemma 1 *[53]. If $h(t) \in C^1([0,+\infty), R)$ denotes a continuously differentiable function, for any $\alpha \in (0,1)$, the following inequality holds almost everywhere:*

$${}_0D_t^\alpha |h(t)| \leq sign(h(t))\, {}_0D_t^\alpha h(t).$$

Lemma 2 *[54]. Let $x(t) \in R^n$ be a vector of differentiable functions. Then, for $t \geq t_0$, the following relationship holds*

$$\frac{1}{2}\, {}_{t_0}D_t^\alpha x^T(t) P x(t) \leq x^T(t) P\, {}_{t_0}D_t^\alpha x(t) \qquad \forall \alpha \in (0,1],$$

where $P \in R^{n\times n}$ is a positive definite matrix.

Lemma 3 *[55]. For any vectors $x, y \in R^n$ and a positive definite matrix $Q \in R^{n\times n}$, the following inequality holds:*

$$2x^T y \leq x^T Q x + y^T Q^{-1} y.$$

Lemma 4 *[56]. (Fractional Halanay inequality) If the continuous function $u(t) > 0, t \in R$, and*

$$\begin{cases} {}_0D_t^\alpha u(t) \leq c_0 + c_3 u(t) + c_4 \sup_{t-\tau(t)\leq\xi\leq t} u(\xi), & t \geq 0, \\ u(t) = |\psi(t)|, t \leq 0, \end{cases}$$

where $0 < \alpha < 1$, $\psi(t)$ is a bounded and continuous function, the coefficients c_0, c_3, c_4 satisfy that $c_0, c_4 \geq 0, c_3 < 0$, and $-\sigma \leq t - \tau(t) \leq t$. Let $M_0 = \sup_{-\sigma\leq\xi\leq 0} |\psi(\xi)|$ and $u_0 = |\psi(0)|$. If $c_3 + c_4 < 0$, then we have

$$u(t) \leq \frac{c_3}{c_3+c_4} u_0 - \frac{c_0}{c_3+c_4} + M_0, \quad t \geq 0.$$

Furthermore, if $lim_{t\to+\infty}(t-\tau(t)) = +\infty$, then for any given $\varepsilon > 0$, there exists $t_* = t_*(M_0, \varepsilon) > 0$ such that

$$u(t) \leq -\frac{c_0}{c_3+c_4} + \varepsilon, \quad t \geq t_*.$$

Lemma 5 *[57]. (Schur's Complement) The linear matrix inequality (LMI)*

$$S = \begin{pmatrix} S_{11} & S_{12} \\ S_{12}^T & S_{22} \end{pmatrix} < 0$$

is equivalent to any one of the following two conditions:

$$(i) \quad S_{11} < 0, \qquad S_{22} - S_{12}^T S_{11}^{-1} S_{12} < 0,$$

$$(ii) \quad S_{22} < 0, \qquad S_{11} - S_{12} S_{22}^{-1} S_{12}^T < 0,$$

where $S_{11} = S_{11}^T$, $S_{22} = S_{22}^T$.

2.2 Problem formulation

In this paper, we consider a class of delayed FMNNs as drive system, which is described by

$$ {}_0D_t^{\alpha} x_i(t) = -c_i x_i(t) + \sum_{j=1}^{n} a_{ij}(x_j(t)) f_j(x_j(t)) + \sum_{j=1}^{n} b_{ij}(x_j(t-\tau)) g_j(x_j(t-\tau)), \tag{1} $$

where $i = 1, 2, \ldots, n$, n is the number of neurons; $0 < \alpha < 1$ is the fractional order; $c_i > 0$ denotes the self-feedback connection weight; $x_i(t)$ is the voltage of the capacitor C_i; $f_j(\cdot)$, $g_j(\cdot)$ denote the activation functions satisfying $f_j(0) = g_j(0) = 0$; τ is the time delay; $a_{ij}(x_j(t))$ and $b_{ij}(x_j(t-\tau))$ are memristive connection weights, which are defined by

$$ a_{ij}(x_j(t)) = \frac{W_{fij}}{C_i} \times \delta_{ij}, $$

$$ b_{ij}(x_j(t-\tau)) = \frac{W_{gij}}{C_i} \times \delta_{ij}, $$

in which $\delta_{ij} = 1$, if $i \neq j$ holds, otherwise, $\delta_{ij} = -1$, W_{fij} and W_{gij} denote the memductance of memristors R_{fij} and R_{gij} respectively, and C_i denotes the capacitance of the capacitor C_i. In [58], it has been shown that memristor needs to exhibit only two sufficiently distinct equilibrium states since digital computer applications require only two memory states. Hence, based on the pinched hysteresis curves, memristive connection weights can be simply represented as

$$ a_{ij}(x_j(t)) = \begin{cases} a_{ij}^{*}, & |x_j(t)| < T_{xj} \\ a_{ij}^{**}, & |x_j(t)| > T_{xj} \end{cases}, \quad b_{ij}(x_j(t-\tau)) = \begin{cases} b_{ij}^{*}, & |x_j(t-\tau)| < T_{xj} \\ b_{ij}^{**}, & |x_j(t-\tau)| > T_{xj} \end{cases}, $$

for $i, j = 1, 2, \ldots, n$, where the switching jumps $T_{xj} > 0$, and a_{ij}^{*}, a_{ij}^{**}, b_{ij}^{*}, b_{ij}^{**} are all constants. The initial condition of system (1) is assumed to be $x_i(s) = \vartheta_{xi}(s)$, $s \in [-\tau, 0]$, where $\vartheta_{xi}(s) \in C([-\tau, 0], R)$.

Remark 1 *FMNNs system (1) can be considered as a switched system, which consists of 2^n subsystems (FNNs) and it may exhibit some complex nonlinear dynamics. On the face of it, the switching jumps can not change the values of the memristive connection weights. Nevertheless, switching jumps play an important role in the dynamics of system (1) since they can not only affect the running time but also determine the switching order of the subsystems that system (1) goes through. Different from traditional switched systems, it is worthwhile to notice that the switching laws of system (1) are uncertain, because the switching patterns of memristive connection weights $a_{ij}(x_j(t))$ and $b_{ij}(x_j(t-\tau))$ depend on the initial values, the states, as well as the switching jumps T_{xj}.*

Accordingly, the response system is described by

$$ {}_0D_t^{\alpha} y_i(t) = -c_i y_i(t) + \sum_{j=1}^{n} a_{ij}(y_j(t)) f_j(y_j(t)) + \sum_{j=1}^{n} b_{ij}(y_j(t-\tau)) g_j(y_j(t-\tau)) + u_i(t), \tag{2} $$

where $i = 1, 2, \ldots, n$, $c_i > 0$ denotes the self-feedback connection weight; $y_i(t)$ corresponds to the state variable connected with the ith neuron; $u_i(t)$ is the control input to be designed later; $a_{ij}(y_j(t))$ and $b_{ij}(y_j(t-\tau))$ are memristive connection weights, which are represented by

$$ a_{ij}(y_j(t)) = \begin{cases} a_{ij}^{*}, & |y_j(t)| < T_{yj} \\ a_{ij}^{**}, & |y_j(t)| > T_{yj} \end{cases}, \quad b_{ij}(y_j(t-\tau)) = \begin{cases} b_{ij}^{*}, & |y_j(t-\tau)| < T_{yj} \\ b_{ij}^{**}, & |y_j(t-\tau)| > T_{yj} \end{cases}, $$

for $i,j=1,2,\ldots,n$, where the switching jumps $T_{yj}>0$. The initial condition of system (2) is assumed to be $y_i(s)=\vartheta_{yi}(s)$, $s\in[-\tau,0]$, where $\vartheta_{yi}(s)\in C([-\tau,0],R)$.

Since $a_{ij}(x_j(t))$ and $b_{ij}(x_j(t-\tau))$, $a_{ij}(y_j(t))$ and $b_{ij}(y_j(t-\tau))$ are discontinuous at the switching jumps T_{xj}, T_{yj}, respectively, the solutions of drive and response systems should be handled in Filippov's sense. Denote $\bar{a}_{ij}=\max\{a^*_{ij},a^{**}_{ij}\}$, $\underline{a}_{ij}=\min\{a^*_{ij},a^{**}_{ij}\}$, $\bar{b}_{ij}=\max\{b^*_{ij},b^{**}_{ij}\}$, $\underline{b}_{ij}=\min\{b^*_{ij},b^{**}_{ij}\}$. For system (1), define the multi-valued maps as follows

$$K[a_{ij}(x_j(t))]=\begin{cases}a^*_{ij}, & |x_j(t)|<T_{xj}\\ co\{a^*_{ij},a^{**}_{ij}\}, & |x_j(t)|=T_{xj}\\ a^{**}_{ij}, & |x_j(t)|>T_{xj}\end{cases},\quad K[b_{ij}(x_j(t-\tau))]=\begin{cases}b^*_{ij}, & |x_j(t-\tau)|<T_{xj}\\ co\{b^*_{ij},b^{**}_{ij}\}, & |x_j(t-\tau)|=T_{xj}\\ b^{**}_{ij}, & |x_j(t-\tau)|>T_{xj}\end{cases},$$

for $i,j=1,2,\cdots n$. Clearly, we have $co\{a^*_{ij},a^{**}_{ij}\}=[\underline{a}_{ij},\bar{a}_{ij}]$, $co\{b^*_{ij},b^{**}_{ij}\}=[\underline{b}_{ij},\bar{b}_{ij}]$.

For $i=1,2,\cdots,n$, it is evident that the set-valued map

$$x_i(t)\mapsto -c_ix_i(t)+\sum_{j=1}^{n}K[a_{ij}(x_j(t))]f_j(x_j(t))+\sum_{j=1}^{n}K[b_{ij}(x_j(t-\tau))]g_j(x_j(t-\tau)),$$

is nonempty, compact and convex. Furthermore, it is upper semi-continuous [59].

A solution $x(t)=(x_1(t),x_2(t),\cdots,x_n(t))^T$ in Filippov's sense of system (1) with initial condition $x(t)=\phi(t)\in C([-\tau,0),R^n)$ is defined as an absolutely continuous function on any compact interval of $[0,+\infty)$, and satisfies

$${}_0D_t^{\alpha}x_i(t)\in -c_ix_i(t)+\sum_{j=1}^{n}K[a_{ij}(x_j(t))]f_j(x_j(t))+\sum_{j=1}^{n}K[b_{ij}(x_j(t-\tau))]g_j(x_j(t-\tau)).\tag{3}$$

By the theories of set-valued maps [52] and fractional-order differential inclusions [51], it follows that system (1) is equivalent to the fractional-order differential inclusion (3) within the mathematical framework of Filippov solution.

Furthermore, by the measurable selection theorem [60], there exist measurable functions $\gamma_{ij}(x_j(t))\in K[a_{ij}(x_j(t))]$, $\rho_{ij}(x_j(t-\tau))\in K[b_{ij}(x_j(t-\tau))]$, such that

$${}_0D_t^{\alpha}x_i(t)=-c_ix_i(t)+\sum_{j=1}^{n}\gamma_{ij}(x_j(t))f_j(x_j(t))+\sum_{j=1}^{n}\rho_{ij}(x_j(t-\tau))g_j(x_j(t-\tau)).\tag{4}$$

Similarly, for system (2), define

$$K[a_{ij}(y_j(t))]=\begin{cases}a^*_{ij}, & |y_j(t)|<T_{yj}\\ co\{a^*_{ij},a^{**}_{ij}\}, & |y_j(t)|=T_{yj}\\ a^{**}_{ij}, & |y_j(t)|>T_{yj}\end{cases},\quad K[b_{ij}(y_j(t-\tau))]=\begin{cases}b^*_{ij}, & |y_j(t-\tau)|<T_{yj}\\ co\{b^*_{ij},b^{**}_{ij}\}, & |y_j(t-\tau)|=T_{yj}\\ b^{**}_{ij}, & |y_j(t-\tau)|>T_{yj}\end{cases},$$

where $i,j=1,2,\ldots,n$, $co\{a^*_{ij},a^{**}_{ij}\}=[\underline{a}_{ij},\bar{a}_{ij}]$, $co\{b^*_{ij},b^{**}_{ij}\}=[\underline{b}_{ij},\bar{b}_{ij}]$.

Then, system (2) is equivalent to

$${}_0D_t^{\alpha}y_i(t)\in -c_iy_i(t)+\sum_{j=1}^{n}K[a_{ij}(y_j(t))]f_j(y_j(t))+\sum_{j=1}^{n}K[b_{ij}(y_j(t-\tau))]g_j(y_j(t-\tau))+u_i(t),\tag{5}$$

Similarly, there exist measurable functions $\gamma_{ij}(y_j(t))\in K[a_{ij}(y_j(t))]$ and $\rho_{ij}(y_j(t-\tau))\in K[b_{ij}(y_j(t-\tau))]$ such that

$$_0D_t^{\alpha} y_i(t) = -c_i y_i(t) + \sum_{j=1}^{n} \gamma_{ij}(y_j(t)) f_j(y_j(t)) + \sum_{j=1}^{n} \rho_{ij}(y_j(t-\tau)) g_j(y_j(t-\tau)) + u_i(t). \tag{6}$$

In order to address the synchronization issue of drive-response systems (1)-(2) or (4)-(6), in what follows, we introduce the controller and derive the error system.

Let $e_i(t) = y_i(t) - x_i(t)$ be the synchronization error, and the control input is designed as

$$u_i(t) = -k_i e_i(t), \tag{7}$$

where $k_i > 0$, $i = 1, 2, \ldots, n$. Then, the error system can be obtained from (4) and (6), represented by

$$\begin{aligned} _0D_t^{\alpha} e_i(t) = & -(c_i + k_i) e_i(t) + \sum_{j=1}^{n} [\gamma_{ij}(y_j(t)) f_j(y_j(t)) - \gamma_{ij}(x_j(t)) f_j(x_j(t))] \\ & + \sum_{j=1}^{n} [\rho_{ij}(y_j(t-\tau)) g_j(y_j(t-\tau)) - \rho_{ij}(x_j(t-\tau)) g_j(x_j(t-\tau))]. \end{aligned} \tag{8}$$

The initial condition of error system (8) is defined by

$$e_i(s) = \phi_i(s), \qquad -\tau \leq s \leq 0,$$

where $\phi_i(s) = \vartheta_{yi}(s) - \vartheta_{xi}(s) \in C([-\tau, 0], R)$.

Denote $x(t) = [x_1(t), x_2(t), \ldots, x_n(t)]^T$, $y(t) = [y_1(t), y_2(t), \ldots, y_n(t)]^T$, $e(t) = [e_1(t), e_2(t), \ldots, e_n(t)]^T$, and $\phi(s) = [\phi_1(s), \phi_2(s), \ldots, \phi_n(s)]^T$.

In order to ensure the existence of solution of system (1) or differential inclusion (3), the following assumption should be imposed on the activation functions $f_j(\cdot)$ and $g_j(\cdot)$.

Assumption 1 *The activation functions $f_j(\cdot)$ and $g_j(\cdot)$ are Lipschitz-continuous with Lipschitz constants $L_j, M_j > 0$, respectively, i.e.,*

$$|f_j(u) - f_j(v)| \leq L_j |u - v|,$$
$$|g_j(u) - g_j(v)| \leq M_j |u - v|,$$

for all $u, v \in R$, and $j = 1, 2, \ldots, n$.

In [28, 40], the authors have demonstrated that the traditional linear feedback controller cannot realize complete synchronization between two identical MNNs or FMNNs with different initial values by numerical simulation. In this paper, we will explore this question in theory. In fact, the mismatches between the initial values or the switching jumps can cause the mismatches between the connection weights. As a consequence, it will give rise to undesired synchronization error between the neuronal states. In order to describe this phenomenon and to analyze the influence of parameter mismatches on synchronization error, we introduce the concepts of ASTI and SSTI in what follows.

Definition 5 *The drive-response systems (1)-(2) are said to stay in* **asynchronous switching time interval (ASTI)***, if there exists a time interval (t_r', s_r') such that*

$$a_{ij}(x_j(t)) \neq a_{ij}(y_j(t)) \quad or \quad b_{ij}(x_j(t-\tau)) \neq b_{ij}(y_j(t-\tau)), \qquad for \quad t \in (t_r', s_r').$$

The drive-response systems (1)-(2) are said to stay in **synchronous switching time interval (SSTI)***, if there exists a time interval (s_r', t_{r+1}') such that*

$$a_{ij}(x_j(t)) = a_{ij}(y_j(t)) \quad and \quad b_{ij}(x_j(t-\tau)) = b_{ij}(y_j(t-\tau)), \qquad for \quad t \in (s_r', t_{r+1}'),$$

where $i, j = 1, 2, \cdots, n$, $r = 0, 1, 2, \cdots$.

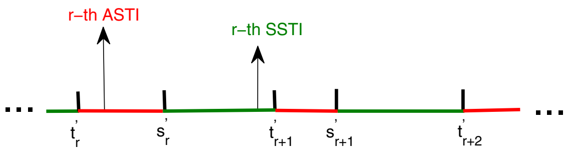

Fig. 1. Distributions of ASTI and SSTI.

As shown in Fig. 1, ASTI and SSTI will alternately appear during the process of dynamical evolution of FMNNs. Obviously, when $t \in (t_r^{'}, s_r^{'})$, the drive-response systems become two non-identical systems. And when $t \in (s_r^{'}, t_{r+1}^{'})$, the drive-response systems become two identical systems.

In particular, for drive-response FMNNs (1)-(2), assume that $\vartheta_x(s) \neq \vartheta_y(s)$ and $T_{xj} = T_{yj}$, we claim that it would be impossible to eliminate the error caused only by the initial values. The explanation is as follows. Although there may be some SSTI, denoted by $(s_r^{'}, t_{r+1}^{'})$, (without loss of generality, suppose it is $(s_0^{'}, t_1^{'})$, namely, drive-response systems (1)-(2) are identical from the very beginning), it is impossible to achieve complete synchronization in this interval because it has been shown that finite-time stability does not exist for fractional-order nonlinear systems based on continuous controller [61]. Thus, the remaining error, which is not completely eliminated from $(s_0^{'}, t_1^{'})$ would lead to a situation that $x_j(t)$ and $y_j(t)$ or $x_j(t-\tau)$ and $y_j(t-\tau)$ could not simultaneously arrive at the switching jumps T_{xj}. It implies that the drive and response systems can not switch synchronously and this will lead to the occurrence of $a_{ij}(x_j(t)) \neq a_{ij}(y_j(t))$ or $b_{ij}(x_j(t-\tau)) \neq b_{ij}(y_j(t-\tau))$. That is, the ASTI will appear. In ASTI, new synchronization error will arise from the mismatches between connection weights. Similarly, the synchronization error can not be completely eliminated in this finite time interval. Note that for the rest of time ASTI and SSTI may alternately appear. In a word, complete synchronization cannot be achieved by linear feedback controller since there always exists error generated by the two non-identical subsystems in ASTI.

From above analysis, one can see that ASTI has hidden but importance influence on the synchronization of FMNNs. In fact, no matter whether the initial values are identical or not, complete synchronization may fail to achieve for systems (1)-(2) via linear feedback if the switching jumps $T_{xj} \neq T_{yj}$, i.e. $\Delta T = |T_{xj} - T_{yj}| \neq 0$, since ASTI does exist. In this case, quasi-synchronization will be achieved based on linear feedback control, which is defined as follows.

Definition 6 *[39]. Drive-response systems (4)-(6) are said to achieve quasi-synchronization with error bound $\varepsilon > 0$ if there exists a compact set M such that for any $\phi(s) \in C([-\tau, 0], \mathbf{R}^n)$, the error $e(t) = y(t) - x(t)$ converges to $M = \{||e(t)|| \leq \varepsilon\}$ as t goes to infinity.*

Before introducing the main results, we first prove the following lemma. Define $a_{ij}^u = \max\{|a_{ij}^*|, |a_{ij}^{**}|\}$, $b_{ij}^u = \max\{|b_{ij}^*|, |b_{ij}^{**}|\}$, $T_{\max} = \max\{T_{xj}, T_{yj}\}$, $\Delta a_{ij} = a_{ij}^* - a_{ij}^{**}$, $\Delta b_{ij} = b_{ij}^* - b_{ij}^{**}$.

Lemma 6 *Under **Assumption 1**, the following inequalities hold:*

(i)

$$|K[a_{ij}(y_j(t))]f_j(y_j(t)) - K[a_{ij}(x_j(t))]f_j(x_j(t))| \leq a_{ij}^u L_j |e_j(t)| + |\Delta a_{ij}| L_j T_{\max},$$

(ii)

$$|K[b_{ij}(y_j(t-\tau))]g_j(y_j(t-\tau)) - K[b_{ij}(x_j(t-\tau))]g_j(x_j(t-\tau))| \leq b_{ij}^u M_j |e_j(t-\tau)| + |\Delta b_{ij}| M_j T_{\max},$$

for $i, j = 1, 2, \ldots, n$, that is, for any $\gamma_{ij}(x_j(t)) \in K[a_{ij}(x_j(t))]$, $\gamma_{ij}(y_j(t)) \in K[a_{ij}(y_j(t))]$, $\rho_{ij}(x_j(t-\tau)) \in K[b_{ij}(x_j(t-\tau))]$ and $\rho_{ij}(y_j(t-\tau)) \in K[b_{ij}(y_j(t-\tau))]$, we have

$$|\gamma_{ij}(y_j(t))f_j(y_j(t)) - \gamma_{ij}(x_j(t))f_j(x_j(t))| \leq a_{ij}^u L_j |e_j(t)| + |\Delta a_{ij}| L_j T_{\max},$$

$$|\rho_{ij}(y_j(t-\tau))g_j(y_j(t-\tau)) - \rho_{ij}(x_j(t-\tau))g_j(x_j(t-\tau))| \leq b_{ij}^u M_j |e_j(t-\tau)| + |\Delta b_{ij}| M_j T_{\max},$$

for $i, j = 1, 2, \ldots, n$.

Proof For any given $i, j = 1, 2, \ldots, n$, and $x_j, y_j \in R$, we have the following four cases.

Case 1: If $|x_j(t)| < T_{xj}$, $|y_j(t)| < T_{yj}$, then

$$\begin{aligned} |K[a_{ij}(y_j(t))]f_j(y_j(t)) - K[a_{ij}(x_j(t))]f_j(x_j(t))| &= |a_{ij}^* f_j(y_j(t)) - a_{ij}^* f_j(x_j(t))| \\ &\leq |a_{ij}^*||f_j(y_j(t)) - f_j(x_j(t))| \\ &\leq a_{ij}^u L_j |e_j(t)|. \end{aligned}$$

Case 2: If $|x_j(t)| > T_{xj}$, $|y_j(t)| > T_{yj}$, then

$$\begin{aligned} |K[a_{ij}(y_j(t))]f_j(y_j(t)) - K[a_{ij}(x_j(t))]f_j(x_j(t))| &= |a_{ij}^{**} f_j(y_j(t)) - a_{ij}^{**} f_j(x_j(t))| \\ &\leq |a_{ij}^{**}||f_j(y_j(t)) - f_j(x_j(t))| \\ &\leq a_{ij}^u L_j |e_j(t)|. \end{aligned}$$

Case 3: If $|x_j(t)| \leq T_{xj}$, $|y_j(t)| \geq T_{yj}$, then

$$\begin{aligned} |K[a_{ij}(y_j(t))]f_j(y_j(t)) - K[a_{ij}(x_j(t))]f_j(x_j(t))| &= |a_{ij}^{**} f_j(y_j(t)) - a_{ij}^* f_j(x_j(t))| \\ &= |a_{ij}^{**}[f_j(y_j(t)) - f_j(x_j(t))] + (a_{ij}^{**} - a_{ij}^*) f_j(x_j(t))| \\ &\leq a_{ij}^u L_j |e_j(t)| + |a_{ij}^* - a_{ij}^{**}| L_j |x_j(t)| \\ &\leq a_{ij}^u L_j |e_j(t)| + |\Delta a_{ij}| L_j T_{\max}. \end{aligned}$$

Case 4: If $|x_j(t)| \geq T_{xj}$, $|y_j(t)| \leq T_{yj}$, then

$$\begin{aligned} |K[a_{ij}(y_j(t))]f_j(y_j(t)) - K[a_{ij}(x_j(t))]f_j(x_j(t))| &= |a_{ij}^* f_j(y_j(t)) - a_{ij}^{**} f_j(x_j(t))| \\ &= |a_{ij}^{**}[f_j(y_j(t)) - f_j(x_j(t))] + (a_{ij}^* - a_{ij}^{**}) f_j(y_j(t))| \\ &\leq a_{ij}^u L_j |e_j(t)| + |a_{ij}^* - a_{ij}^{**}| L_j |y_j(t)| \\ &\leq a_{ij}^u L_j |e_j(t)| + |\Delta a_{ij}| L_j T_{\max}. \end{aligned}$$

Therefore, we can obtain

$$|K[a_{ij}(y_j(t))]f_j(y_j(t)) - K[a_{ij}(x_j(t))]f_j(x_j(t))| \leq a_{ij}^u L_j |e_j(t)| + |\Delta a_{ij}| L_j T_{\max}.$$

Similarly, we have

$$|K[b_{ij}(y_j(t-\tau))]g_j(y_j(t-\tau)) - K[b_{ij}(x_j(t-\tau))]g_j(x_j(t-\tau))| \leq b_{ij}^u M_j |e_j(t-\tau)| + |\Delta b_{ij}| M_j T_{\max}.$$

The proof of the lemma is complete.

3 Main results

In this section, by constructing some appropriate Lyapunov functionals and employing the linear matrix inequality (LMI) technique, some conditions which ensure the quasi-synchronization of drive-response systems (1)-(2) are derived based on linear feedback control.

Theorem 1 Suppose **Assumption 1** holds and that the following algebraic condition

$$\min_{1\le i\le n}\left\{c_i+k_i-\sum_{j=1}^{n}a_{ji}^{u}L_i\right\}>\max_{1\le i\le n}\left\{\sum_{j=1}^{n}b_{ji}^{u}M_i\right\}$$

is satisfied, then drive-response systems (1)-(2) with the control law (7) achieve quasi-synchronization with error bound $\frac{\theta}{\lambda-\mu}$, where $\lambda=\min_{1\le i\le n}\left\{c_i+k_i-\sum_{j=1}^{n}a_{ji}^{u}L_i\right\}$, $\mu=\max_{1\le i\le n}\left\{\sum_{j=1}^{n}b_{ji}^{u}M_i\right\}$, $\theta=\sum_{i=1}^{n}\sum_{j=1}^{n}|\Delta a_{ij}|L_jT_{\max}+\sum_{i=1}^{n}\sum_{j=1}^{n}|\Delta b_{ij}|M_jT_{\max}$.

Proof. Consider the Lyapunov functional as follows

$$V(t)=\sum_{i=1}^{n}|e_i(t)|.$$

From **Lemma 1**, **Lemma 6** and **Assumption 1**, we obtain

$$\begin{aligned}
D_t^{\alpha}V(t)=D_t^{\alpha}\sum_{i=1}^{n}|e_i(t)|&\le\sum_{i=1}^{n}sign(e_i(t))\,D_t^{\alpha}e_i(t)\\
&=\sum_{i=1}^{n}sign(e_i(t))\Big\{-(c_i+k_i)e_i(t)+\sum_{j=1}^{n}[\gamma_{ij}(y_j(t))f_j(y_j(t))-\gamma_{ij}(x_j(t))f_j(x_j(t))]\\
&\quad+\sum_{j=1}^{n}[\rho_{ij}(y_j(t-\tau))g_j(y_j(t-\tau))-\rho_{ij}(x_j(t-\tau))g_j(x_j(t-\tau))]\Big\}\\
&\le-\sum_{i=1}^{n}(c_i+k_i)|e_i(t)|+\sum_{i=1}^{n}\sum_{j=1}^{n}a_{ij}^{u}L_j|e_j(t)|+\sum_{i=1}^{n}\sum_{j=1}^{n}b_{ij}^{u}M_j|e_j(t-\tau)|\\
&\quad+\sum_{i=1}^{n}\sum_{j=1}^{n}|\Delta a_{ij}|L_jT_{\max}+\sum_{i=1}^{n}\sum_{j=1}^{n}|\Delta b_{ij}|M_jT_{\max}\\
&=-\sum_{i=1}^{n}(c_i+k_i-\sum_{j=1}^{n}a_{ji}^{u}L_i)|e_i(t)|+\sum_{i=1}^{n}\sum_{j=1}^{n}b_{ji}^{u}M_i|e_i(t-\tau)|\\
&\quad+\sum_{i=1}^{n}\sum_{j=1}^{n}|\Delta a_{ij}|L_jT_{\max}+\sum_{i=1}^{n}\sum_{j=1}^{n}|\Delta b_{ij}|M_jT_{\max}.
\end{aligned}$$

Let $\lambda=\min_{1\le i\le n}\left\{c_i+k_i-\sum_{j=1}^{n}a_{ji}^{u}L_i\right\}$, $\mu=\max_{1\le i\le n}\left\{\sum_{j=1}^{n}b_{ji}^{u}M_i\right\}$, $\theta=\sum_{i=1}^{n}\sum_{j=1}^{n}|\Delta a_{ij}|L_j\times T_{\max}+\sum_{i=1}^{n}\sum_{j=1}^{n}|\Delta b_{ij}|M_jT_{\max}$. Then, we have

$$\begin{aligned}
D_t^{\alpha}V(t)&\le-\lambda\sum_{i=1}^{n}|e_i(t)|+\mu\sum_{i=1}^{n}|e_i(t-\tau)|+\theta\\
&=-\lambda V(t)+\mu V(t-\tau)+\theta
\end{aligned}$$

$$\leq -\lambda V(t) + \mu \sup_{t-\tau\leq s\leq t} V(s) + \theta.$$

From the condition of **Theorem 1**, we obtain $\lambda - \mu > 0$. Then, based on **Lemma 4**, we have

$$||e(t)||_1 \leq \frac{\theta}{\lambda - \mu}, \qquad t \to +\infty.$$

Thus, we conclude that the error system (8) converges to the region D, where

$$D = \left\{ e(t) : ||e(t)||_1 \leq \frac{\theta}{\lambda - \mu} \right\}, \qquad t \to +\infty,$$

which implies that drive system (1) and response system (2) achieve quasi-synchronization with error bound $\frac{\theta}{\lambda-\mu}$. This completes the proof.

Theorem 2 Suppose **Assumption 1** holds and that there exist diagonal matrices $P > 0$, $Q_1 > 0$, $Q_2 > 0$, G, and two scalars $\lambda > 0$, $\mu > 0$, such that the LMIs
(i)

$$\begin{bmatrix} -2PC - 2G + P\tilde{A}L + L\tilde{A}^T P + \lambda P & P\widetilde{B} & P \\ * & -Q_1 & 0 \\ * & * & -Q_2 \end{bmatrix} < 0,$$

(ii)

$$Q_1 M^2 - \mu P < 0,$$

(iii)

$$\lambda - \mu > 0,$$

are satisfied, then drive-response systems (1)-(2) with the control law (7) achieve quasi-synchronization with error bound $\sqrt{\frac{\theta}{\min(p_i)(\lambda-\mu)}}$, where $C = diag(c_1, c_2, \ldots, c_n)$, $\tilde{A} = (a_{ij}^u)_{n\times n}$, $\tilde{B} = (b_{ij}^u)_{n\times n}$, $M = diag(M_1, M_2, \ldots, M_n)$, $L = diag(L_1, L_2, \ldots, L_n)$, $\theta = H^T Q_2 H$, $H = \Delta A L \tilde{T}_{\max} + \Delta B M \tilde{T}_{\max}$, $\tilde{T}_{\max} = (T_{\max}, T_{\max}, \ldots, T_{\max})^T$, $\Delta A = (|\Delta a_{ij}|)_{n\times n}$, $\Delta B = (|\Delta b_{ij}|)_{n\times n}$. Moreover, the linear feedback gain is given by $K = P^{-1}G$, where $K = diag(k_1, k_2, \ldots, k_n)$ and $P = diag(p_1, p_2, \ldots, p_n)$.

Proof. Consider the Lyapunov functional as follows

$$V(t) = |e(t)|^T P |e(t)|. \tag{9}$$

where $|e(t)| = (|e_1(t)|, |e_2(t)|, \ldots, |e_n(t)|)^T$, $P = diag(p_1, p_2, \ldots, p_n)$.

From **Lemma 1-Lemma 3**, **Lemma 6** and **Assumption 1**, we have

$$\begin{aligned}
{}_0D_t^{\alpha} V(t) &\leq 2|e(t)|^T P \, {}_0D_t^{\alpha} |e(t)| \\
&= 2\sum_{i=1}^{n} |e_i(t)| p_i \, {}_0D_t^{\alpha} |e_i(t)| \\
&\leq 2\sum_{i=1}^{n} |e_i(t)| p_i sign(e_i(t)) \, {}_0D_t^{\alpha} e_i(t) \\
&= 2\sum_{i=1}^{n} |e_i(t)| p_i sign(e_i(t) \big\{ -(c_i + k_i) e_i(t) + \sum_{j=1}^{n} [\gamma_{ij}(y_j(t)) f_j(y_j(t)) - \gamma_{ij}(x_j(t)) f_j(x_j(t))]
\end{aligned}$$

$$
\begin{aligned}
&+\sum_{j=1}^{n}[\rho_{ij}(y_j(t-\tau))g_j(y_j(t-\tau))-\rho_{ij}(x_j(t-\tau))g_j(x_j(t-\tau))]\}\\
&\leq -2\sum_{i=1}^{n}|e_i(t)|p_i(c_i+k_i)|e_i(t)|+2\sum_{i=1}^{n}\sum_{j=1}^{n}|e_i(t)|p_i|\gamma_{ij}(y_j(t))f_j(y_j(t))-\gamma_{ij}(x_j(t))f_j(x_j(t))|\\
&+2\sum_{i=1}^{n}\sum_{j=1}^{n}|e_i(t)|p_i|\rho_{ij}(y_j(t-\tau))g_j(y_j(t-\tau))-\rho_{ij}(x_j(t-\tau))g_j(x_j(t-\tau))|\\
&\leq -2\sum_{i=1}^{n}|e_i(t)|p_i(c_i+k_i)|e_i(t)|+2\sum_{i=1}^{n}\sum_{j=1}^{n}|e_i(t)|p_i(a_{ij}^{u}L_j|e_j(t)|+|\Delta a_{ij}|L_jT_{\max})\\
&+2\sum_{i=1}^{n}\sum_{j=1}^{n}|e_i(t)|p_i(b_{ij}^{u}M_j|e_j(t-\tau)|+|\Delta b_{ij}|M_jT_{\max})\\
&=-2\sum_{i=1}^{n}|e_i(t)|p_i(c_i+k_i)|e_i(t)|+2\sum_{i=1}^{n}\sum_{j=1}^{n}|e_i(t)|p_ia_{ij}^{u}L_j|e_j(t)|+2\sum_{i=1}^{n}\sum_{j=1}^{n}|e_i(t)|p_i|\Delta a_{ij}|L_jT_{\max}\\
&+2\sum_{i=1}^{n}\sum_{j=1}^{n}|e_i(t)|p_ib_{ij}^{u}M_j|e_j(t-\tau)|+2\sum_{i=1}^{n}\sum_{j=1}^{n}|e_i(t)|p_i|\Delta b_{ij}|M_jT_{\max}\\
&=-2|e(t)|^TP(C+K)|e(t)|+2|e(t)|^TP\tilde{A}L|e(t)|+2|e(t)|^TP\tilde{B}M|e(t-\tau)|+2|e(t)|^TPH\\
&\leq -2|e(t)|^TP(C+K)|e(t)|+2|e(t)|^TP\tilde{A}L|e(t)|+|e(t)|^TP\tilde{B}Q_1^{-1}\tilde{B}^TP|e(t)|\\
&+|e(t-\tau)|^TQ_1M^2|e(t-\tau)|+|e(t)|^TQ_2^{-1}P^2|e(t)|+H^TQ_2H\\
&=|e(t)|^T(-2PC-2PK+P\tilde{A}L+L\tilde{A}^TP+P\tilde{B}Q_1^{-1}\tilde{B}^TP+Q_2^{-1}P^2+\lambda P)|e(t)|\\
&-\lambda|e(t)|^TP|e(t)|+|e(t-\tau)|^T(Q_1M^2-\mu P)|e(t-\tau)|\\
&+\mu|e(t-\tau)|^TP|e(t-\tau)|+H^TQ_2H.
\end{aligned}
$$

By **Lemma 5**, the condition (i) of **Theorem 2** is equivalent to

$$-2PC-2PK+P\tilde{A}L+L\tilde{A}^TP+P\tilde{B}Q_1^{-1}\tilde{B}^TP+Q_2^{-1}P^2+\lambda P<0.$$

Combined with condition (ii) of **Theorem 2**, we obtain

$$
\begin{aligned}
{}_0D_t^{\alpha}V(t)&\leq -\lambda|e(t)|^TP|e(t)|+\mu|e(t-\tau)|^TP|e(t-\tau)|+H^TQ_2H\\
&\leq -\lambda|e(t)|^TP|e(t)|+\mu|e(t-\tau)|^TP|e(t-\tau)|+\theta\\
&=-\lambda V(t)+\mu V(t-\tau)+\theta\\
&\leq -\lambda V(t)+\mu\sup_{t-\tau\leq s\leq t}V(s)+\theta.
\end{aligned}
$$

From the condition (iii) of **Theorem 2**, we get $\lambda-\mu>0$. Based on **Lemma 4**, we have

$$V(t)\leq\frac{\theta}{\lambda-\mu},\qquad t\to+\infty. \tag{10}$$

Note that $V(t)=|e(t)|^TP|e(t)|=\sum_{i=1}^{n}p_i|e_i(t)|^2$. Hence, we have

$$\min(p_i)||e(t)||_2^2\leq V(t)\leq\max(p_i)||e(t)||_2^2. \tag{11}$$

Based on (10) and (11), we obtain

$$\min(p_i)||e(t)||_2^2\leq V(t)\leq\frac{\theta}{\lambda-\mu},\qquad t\to+\infty.$$

Therefore, we obtain

$$||e(t)||_2 \le \sqrt{\frac{\theta}{\min(p_i)(\lambda-\mu)}}, \qquad t \to +\infty.$$

Thus, we can conclude that the error system (8) converges to the region D, where

$$D = \left\{ e(t) : ||e(t)||_2 \le \sqrt{\frac{\theta}{\min(p_i)(\lambda-\mu)}} \right\}, \qquad t \to +\infty,$$

which indicates that drive system (1) and response system (2) achieve quasi-synchronization with an error bound $\sqrt{\frac{\theta}{\min(p_i)(\lambda-\mu)}}$. This completes the proof.

Remark 2 *From **Theorem 1** and **Theorem 2**, it can be seen that the estimated synchronization error bound will increase if the switching jump T_{max} increases. It is worthwhile to note that this is the first time that some synchronization criteria, in which the synchronization error bound explicitly depends on the switching jump $T_{\max}$, are established. Evidently, more information about the memristive connection weights is involved, so the results obtained in this paper extend and improve some existing results on synchronization of FMNNs. In fact, the synchronization error is affected not only by the switching jump T_{max}, but also by the degree of mismatch between the switching jumps. For convenience, the degree of mismatch is defined and denoted by $\Delta T = |T_{xj} - T_{yj}|$. Obviously, ΔT has an immediate impact on the distribution of ASTI. Indeed, ΔT also has a hidden but far-reaching effect on the practical synchronization error. From the above, we know that the error is generated in ASTI, and cannot be completely eliminated by controller (7). Therefore, we declare that practical synchronization error depends heavily on the degree of mismatch ΔT. The influence of ΔT on both ASTI and practical synchronization error would be discussed in a more elaborate way in Section 4.*

Remark 3 *The problem of quasi-synchronization for chaotic systems, integer-order chaotic neural networks or FMNNs has been investigated in [37]-[40]. It should be mentioned that, in order to obtain the main results, the following assumption has been imposed.*
Assumption: *There exists a constant scalar $\delta > 0$ such that*

$$||x(t)|| \le \delta, \qquad -\tau \le t.$$

However, although this assumption is reasonable, the fact is that we have to determine the bound of the trajectories of the chaotic system being considered first before making an estimate of the synchronization error. Generally, it is difficult to obtain such bound in practical application, because the bound depends on the initial values. It means that if the initial value varies, we have to evaluate the bound once again. Obviously, this is inconvenient and time-consuming. To overcome the shortcomings, we remove the above assumption in this paper, that is, we do not require the bound of the chaotic trajectory. Therefore, the quasi-synchronization criteria obtained in this paper improve some relevant results.

Remark 4 *In [23, 28], complete synchronization has been achieved under the controller $u(t) = -Ke(t) - Psign(e(t))$. Note that the term $-Psign(e(t))$ plays an important role in eliminating the error generated in ASTI. In [36], complete synchronization of FMNNs has been achieved via periodically intermittent controller, like $u(t) = \begin{cases} -Ke(t), & nT \le t \le nT + \sigma T, \\ 0, & nT + \sigma T \le t \le (n+1)T, \end{cases}$ where $n = 0, 1, 2, \cdots$, T denotes the control period, and $0 < \sigma < 1$ denotes the control width. However, we claim that the above-mentioned periodically intermittent controller cannot guarantee the achievement of complete synchronization. The underlying* *reason is that the error caused by the parameter mismatches in the ASTI can never be completely eliminated. Therefore, it is important to know under what conditions complete synchronization can be achieved via the periodically intermittent controller. This is still an open problem. And we think the controller* $u(t) = \begin{cases} -Ke(t) - Psign(e(t)), \\ nT \le t \le nT + \sigma T \quad and \quad [t_r^{'}, s_r^{'}] \subseteq [nT, nT + \sigma T], \\ 0, \qquad nT + \sigma T \le t \le (n+1)T, \end{cases}$ *may work. It is not hard to see that under the condition* $[t_r^{'}, s_r^{'}] \subseteq [nT, nT+\sigma T]$*, the undesired error generated in ASTI can be eliminated by* $-Psign(e(t))$*. However, we have to say that it is not an easy thing to ensure that each ASTI* $[t_r^{'}, s_r^{'}]$ *is completely covered by the control interval* $[nT, nT + \sigma T]$ *from the viewpoint of implementation of synchronization. The design of periodically intermittent control is a challenging problem and deserves our further investigation.*

Remark 5 *Owing to the complexity of the definition of fractional derivatives, some traditional analysis methods (e.g. Lyapunov-Krasovskii functionals) for integer-order MNNs [19]-[28] cannot be simply extended and applied to FMNNs. In this paper, considering that the existing LMI-based analysis techniques in [9, 41, 42, 43, 44] are not applicable to delayed fractional-order nonlinear systems, some algebraic and LMIs conditions are developed for delayed FMNNs by constructing appropriate fractional-order Lyapunov functionals and establishing two new inequalities about differential inclusions. Note that it is the first time that some LMI-based conditions are derived for delayed FMNNs. It can be seen that the obtained LMI conditions are general, simple, and effective for analyzing synchronization problem of delayed FMNNs. It is believed that the proposed LMI-based analysis technique in this paper brings new insights into the research of FMNNs.*

4 Numerical simulations

Example 1. Consider drive system (1) with $n = 2$, $\alpha = 0.98$, $f_j(x_j) = g_j(x_j) = tanh(x_j)$, $j = 1, 2$, $\tau = 1$. Take $c_1 = 3.8$, $c_2 = 1.8$, $T_{xj} = 1$, and

$$a_{11}(x_1) = \begin{cases} 2.2, & |x_1| < 1 \\ 2.1, & |x_1| > 1 \end{cases}, a_{12}(x_2) = \begin{cases} -2.1, & |x_2| < 1 \\ -2.2, & |x_2| > 1 \end{cases},$$

$$a_{21}(x_1) = \begin{cases} -0.45, & |x_1| < 1 \\ -0.4, & |x_1| > 1 \end{cases}, a_{22}(x_2) = \begin{cases} 2.65, & |x_2| < 1 \\ 2.7, & |x_2| > 1 \end{cases},$$

$$b_{11}(x_1(t-\tau)) = \begin{cases} -3.9, & |x_1(t-\tau)| < 1 \\ -3.8, & |x_1(t-\tau)| > 1 \end{cases}, b_{12}(x_2(t-\tau)) = \begin{cases} -2.5, & |x_2(t-\tau)| < 1 \\ -2.6, & |x_2(t-\tau)| > 1 \end{cases},$$

$$b_{21}(x_1(t-\tau)) = \begin{cases} -1.8, & |x_1(t-\tau)| < 1 \\ -1.7, & |x_1(t-\tau)| > 1 \end{cases}, b_{22}(x_2(t-\tau)) = \begin{cases} -3.5, & |x_2(t-\tau)| < 1 \\ -3.55, & |x_2(t-\tau)| > 1 \end{cases}.$$

In this example, we will show that it is impossible to eliminate the error caused only by the mismatch between the switching jumps. To better illustrate what happened, we take the extreme case. That is, suppose the drive system and response system have the same initial values and differ only in switching jumps. Hence, the response system (2) is assumed to have the same memristive connection weights as those for drive system but with different switching jumps $T_{yj} = 0.1$. The initial values of the drive system and response system are set to be $\vartheta_x(s) = \vartheta_y(s) = (0.8, -0.5)^T$.

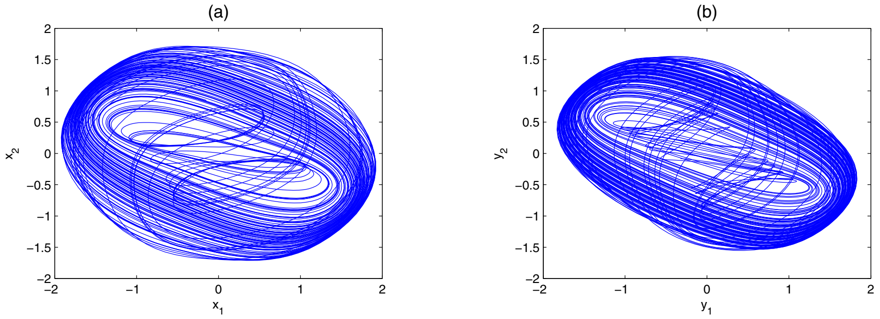

Fig. 2. Chaotic attractors of (a): drive system; (b): response system.

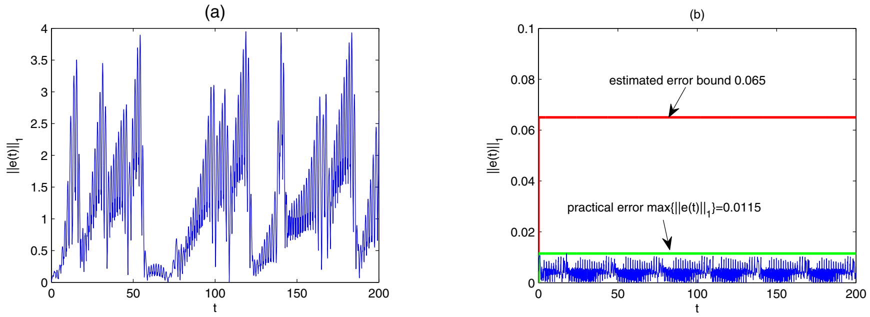

Fig. 3. (a): $||e(t)||_1$ without controller; (b): $||e(t)||_1$ and estimated error with controller (7).

Fig. 2(a) and Fig. 2(b) depict the chaotic attractors of drive system and response system with initial values $\vartheta_x(s) = (0.8, -0.5)^T$ and $\vartheta_y(s) = (0.8, -0.5)^T$, $s \in [-1, 0]$, respectively. When taking $k_1 = 0$, $k_2 = 0$, the evolution of error $||e(t)||_1$ is shown in Fig. 3(a). Choosing $k_1 = 19.25$, $k_2 = 19.25$, by simple calculation, we can obtain $T_{\max} = 1$, $\lambda = \min_{1\le i\le n}\left\{ c_i + k_i - \sum_{j=1}^{n} a_{ji}^{u} L_i \right\} = 16.15$, $\mu = \max_{1\le i\le n}\left\{ \sum_{j=1}^{n} b_{ji}^{u} M_i \right\} = 6.15$, $\theta = \sum_{i=1}^{n}\sum_{j=1}^{n} |\Delta a_{ij}| L_j T_{\max} + \sum_{i=1}^{n}\sum_{j=1}^{n} |\Delta b_{ij}| M_j T_{\max} = 0.65$. According to **Theorem 1**, the drive system and response system achieve quasi-synchronization with estimated error bound $||e(t)||_1 \le \frac{\theta}{\lambda - \mu} = 0.065$, which is verified by Fig. 3(b).

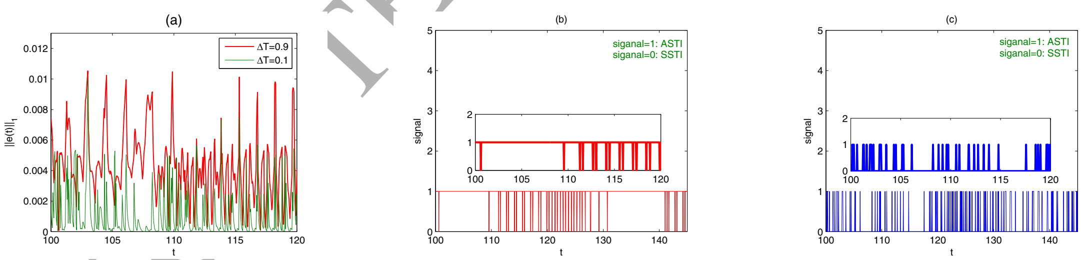

Fig. 4. (a): $||e(t)||_1$ with different ΔT; (b): Distribution of ASTI with $\Delta T = 0.9$; (c): Distribution of ASTI with $\Delta T = 0.1$.

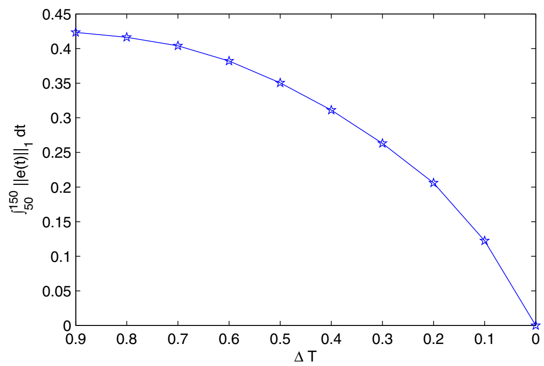

Fig. 5. Trend of $\int_{50}^{150} ||e(t)||_1 dt$ with the decreasing ΔT.

In what follows, we will show the mismatch between the switching jumps T_{xj} and T_{yj} has a tremendous influence on the practical error and the distribution of ASTI. Take $T_{xj} = 1$, $k_1 = 19.25$, $k_2 = 19.25$, when $\Delta T = 0.9$, and $\Delta T = 0.1$, respectively, it is evident that the estimated error bound $||e(t)||_1 \leq 0.065$. Fig. 4(a) shows the evolution of practical synchronization error $||e(t)||_1$ with $\Delta T = 0.9$ and $\Delta T = 0.1$. Fig. 4(b) and Fig. 4(c) show the distribution of ASTI with $\Delta T = 0.9$ and $\Delta T = 0.1$, respectively. We can see that the larger ΔT is, the denser the distribution of ASTI becomes. Take $T_{xj} = 1$, $T_{yj} = 0.1l$ $(l = 1, 2, \ldots, 10)$, Fig. 5 shows the trend of $\int_{50}^{150} ||e(t)||_1 dt$ with the decreasing ΔT. From Fig. 4 and Fig. 5, we can find that ΔT plays an important role in the practical synchronization error and ASTI.

Example 2. Consider drive system (1) with $n = 3$, $\alpha = 0.92$, $f_j(x_j) = g_j(x_j) = tanh(x_j)$, $\tau = 0.9$. Set $c_1 = 2.2$, $c_2 = 1.2$, $c_3 = 1.8$, $s \in [-0.9, 0]$, $T_{xj} = 1$, and

$$a_{11}(x_1) = \begin{cases} 2.2, & |x_1| < 1 \\ 2, & |x_1| > 1 \end{cases}, a_{12}(x_2) = \begin{cases} -2, & |x_2| < 1 \\ -2.1, & |x_2| > 1 \end{cases}, a_{13}(x_3) = \begin{cases} 2, & |x_3| < 1 \\ 1.8, & |x_3| > 1 \end{cases},$$

$$a_{21}(x_1) = \begin{cases} -0.8, & |x_1| < 1 \\ -0.6, & |x_1| > 1 \end{cases}, a_{22}(x_2) = \begin{cases} 5.71, & |x_2| < 1 \\ 5.68, & |x_2| > 1 \end{cases}, a_{23}(x_3) = \begin{cases} 1.15, & |x_3| < 1 \\ 1.1, & |x_3| > 1 \end{cases},$$

$$a_{31}(x_1) = \begin{cases} -4.75, & |x_1| < 1 \\ -4.5, & |x_1| > 1 \end{cases}, a_{32}(x_2) = \begin{cases} -1, & |x_2| < 1 \\ -0.8, & |x_2| > 1 \end{cases}, a_{33}(x_3) = \begin{cases} 1.2, & |x_3| < 1 \\ 1.25, & |x_3| > 1 \end{cases},$$

$$b_{11}(x_1(t-\tau)) = \begin{cases} -4, & |x_1(t-\tau)| < 1 \\ -3.8, & |x_1(t-\tau)| > 1 \end{cases}, b_{12}(x_2(t-\tau)) = \begin{cases} 2.5, & |x_2(t-\tau)| < 1 \\ 2.3, & |x_2(t-\tau)| > 1 \end{cases},$$

$$b_{13}(x_3(t-\tau)) = \begin{cases} -3.2, & |x_3(t-\tau)| < 1 \\ -3.0, & |x_3(t-\tau)| > 1 \end{cases}, b_{21}(x_1(t-\tau)) = \begin{cases} -1.5, & |x_1(t-\tau)| < 1 \\ -1.7, & |x_1(t-\tau)| > 1 \end{cases},$$

$$b_{22}(x_2(t-\tau)) = \begin{cases} -3.6, & |x_2(t-\tau)| < 1 \\ -3.8, & |x_2(t-\tau)| > 1 \end{cases}, b_{23}(x_3(t-\tau)) = \begin{cases} -2.3, & |x_3(t-\tau)| < 1 \\ -2.5, & |x_3(t-\tau)| > 1 \end{cases},$$

$$b_{31}(x_1(t-\tau)) = \begin{cases} 0.3, & |x_1(t-\tau)| < 1 \\ 0.4, & |x_1(t-\tau)| > 1 \end{cases}, b_{32}(x_2(t-\tau)) = \begin{cases} 1.8, & |x_2(t-\tau)| < 1 \\ 2, & |x_2(t-\tau)| > 1 \end{cases},$$

$$b_{33}(x_3(t-\tau)) = \begin{cases} 1.2, & |x_3(t-\tau)| < 1 \\ 1.5, & |x_3(t-\tau)| > 1 \end{cases}.$$

The response system (2) is assumed to have the same parameters as those for drive system but with different switching jumps $T_{yj} = 0.2$.

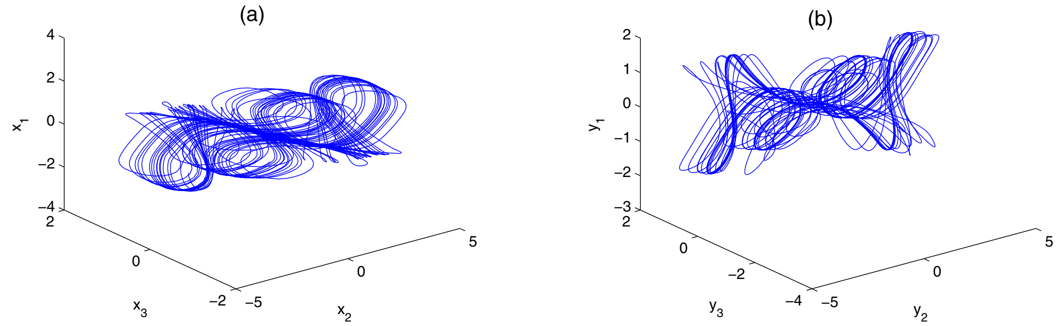

Fig. 6. Chaotic attractors of (a): drive system; (b): response system.

Fig. 6(a) and Fig. 6(b) display the chaotic attractors of drive system and response system with initial values $\vartheta_x(s) = (2, -0.6, 0.2)^T$ and $\vartheta_y(s) = (-2, 5.3, -5)^T$, $s \in [-0.9, 0]$, respectively.

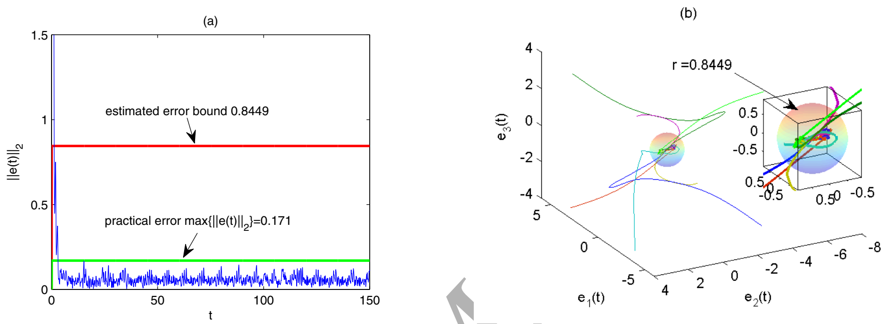

Fig. 7. (a): $||e(t)||_1$ and estimated error with controller (7); (b): Responses of $e_1(t)$, $e_2(t)$, $e_3(t)$ with randomly 7 initial values.

Taking $\lambda = 12$, $\mu = 1.5$, the values of P, G, Q_1, Q_2 are given by solving the LMIs (i) and (ii) in **Theorem 2**. Accordingly, the linear feedback gain can be obtained by solving $K = P^{-1}G$ as follows.

$$P = \begin{bmatrix} 10.5780 & 0 & 0 \\ 0 & 9.7318 & 0 \\ 0 & 0 & 10.1594 \end{bmatrix}, \quad G = \begin{bmatrix} 53.2366 & 0 & 0 \\ 0 & 56.9882 & 0 \\ 0 & 0 & 53.8567 \end{bmatrix},$$

$$Q_1 = \begin{bmatrix} 9.7323 & 0 & 0 \\ 0 & 9.0938 & 0 \\ 0 & 0 & 9.4737 \end{bmatrix}, \quad Q_2 = \begin{bmatrix} 23.0051 & 0 & 0 \\ 0 & 22.5948 & 0 \\ 0 & 0 & 22.8130 \end{bmatrix},$$

$$K = P^{-1}G = \begin{bmatrix} 5.0328 & 0 & 0 \\ 0 & 5.8559 & 0 \\ 0 & 0 & 5.3011 \end{bmatrix}.$$

By simple calculation, we obtain $H = \Delta AL\tilde{T}_{\max} + \Delta BM\tilde{T}_{\max} = (1.1000, 0.8800, 1.1000)^T$, $\theta = ||H^TQ_2H||_2 = 72.9374$. According to **Theorem 2**, the drive system and response system achieve quasi-synchronization with estimated error bound $||e(t)||_2 \leq \sqrt{\frac{\theta}{\min(p_i)(\lambda-\mu)}} = 0.8449$, which is verified by Fig. 7.

5 Conclusions

In this paper, the quasi-synchronization of delayed FMNNs with mismatched switching jumps is investigated. A linear state feedback law is designed, which is simple and easy to implemented. Two improved criteria are developed by dropping the assumption on boundedness of chaotic systems. It is the first time that the dependence of synchronization error bound on switching jumps is identified. In particular, the effect of the degree of mismatch ΔT on the practical synchronization error is discussed. It has been shown that the practical synchronization error and ASTI depend heavily on ΔT. Finally, two numerical examples are given to validate the theoretical results. It is believed that our results are effective and feasible for the design and application of FMNNs.

6 Acknowledgments

This work was supported by the National Natural Science Foundation of China under Grants 61473178, 61473177, 61573008.

References

[1] Lundstrom, B. N., Higgs, M. H., Spain, W. J., & Fairhall, A. L. (2008). Fractional differentiation by neocortical pyramidal neurons. Nature Neuroscience, 11(11), 1335-1342.

[2] Wang, Z., Huang, X., & Shi, G. (2011). Analysis of nonlinear dynamics and chaos in a fractional order financial system with time delay. Computers & Mathematics with Applications, 62(3), 1531-1539.

[3] Tripathi, D., Pandey, S. K., & Das, S. (2010). Peristaltic flow of viscoelastic fluid with fractional Maxwell model through a channel. Applied Mathematics and Computation, 215(10), 3645-3654.

[4] Samko, S. G., Kilbas, A. A., & Marichev, O. I. (1987). Fractional Integrals and Derivatives and Some of Their Applications. Minsk: Naukai Technika.

[5] Westerlund, S., & Ekstam, L. (1994). Capacitor theory. IEEE Transactions on Dielectrics and Electrical Insulation, 1(5), 826-839.

[6] Boroomand, A., & Menhaj, M. (2009). Fractional-order Hopfield neural networks. Lecture notes in computer science, 5506, 883-890.

[7] Huang, X., Zhao, Z., Wang, Z., & Li, Y. (2012). Chaos and hyperchaos in fractional-order cellular neural networks. Neurocomputing, 94, 13-21.

[8] Wang, Z., Wang, X., Li, Y., Huang, X. (2017). Stability and Hopf bifurcation of fractional-order complex-valued single neuron model with time delay. International Journal of Bifurcation and Chaos, 27(13), 1750209.

[9] Zhang, S., Yu, Y., & Yu, J. (2017). LMI conditions for global stability of fractional-order neural networks. IEEE Transactions on Neural Networks and Learning Systems, 28(10), 2423-2433.

[10] Zhang, L., Yang, Y., & Wang, F. (2017). Synchronization analysis of fractional-order neural networks with time-varying delays via discontinuous neuron activations. Neurocomputing. DOI: 10.1016/j.neucom.2017.04.056.

[11] Wu, A., Zeng, Z., & Song, X. (2016). Global Mittag-Leffler stabilization of fractional-order bidirectional associative memory neural networks. Neurocomputing, 177, 489-496.

[12] Ding, Z., & Shen, Y. (2016). Projective synchronization of nonidentical fractional-order neural networks based on sliding mode controller. Neural Networks, 76, 97-105.

[13] Chua, L. (1971). Memristor-the missing circuit element. IEEE Transactions on Circuit Theory, 18(5), 507-519.

[14] Strukov, D. B., Snider, G. S., Stewart, D. R., & Williams, R. S. (2008). The missing memristor found. Nature, 453(7191), 80-83.

[15] Jo, S. H., Chang, T., Ebong, I., Bhadviya, B. B., Mazumder, P., & Lu, W. (2010). Nanoscale memristor device as synapse in neuromorphic systems. Nano letters, 10(4), 1297-1301.

[16] Adhikari, S. P., Yang, C., Kim, H., & Chua, L. O. (2012). Memristor bridge synapse-based neural network and its learning. IEEE Transactions on Neural Networks and Learning Systems, 23(9), 1426-1435.

[17] Itoh, M., & Chua, L. O. (2009). Memristor cellular automata and memristor discrete-time cellular neural networks. International Journal of Bifurcation and Chaos, 19(11), 3605-3656.

[18] Bao, G., & Zeng, Z. (2017). Region stability analysis for switched discrete-time recurrent neural network with multiple equilibria. Neurocomputing, 249, 182-190.

[19] Xin, Y., Li, Y., Cheng, Z., & Huang, X. (2016). Global exponential stability for switched memristive neural networks with time-varying delays. Neural Networks, 80, 34-42.

[20] Zhang, G., & Shen, Y. (2015). Exponential stabilization of memristor-based chaotic neural networks with time-varying delays via intermittent control. IEEE Transactions on Neural Networks and Learning Systems, 26(7), 1431-1441.

[21] Wang, L., Shen, Y., & Zhang, G. (2017). Finite-time stabilization and adaptive control of memristor-based delayed neural networks. IEEE Transactions on Neural Networks and Learning Systems, 28(11), 2648-2659.

[22] Guo, Z., Wang, J., & Yan, Z. (2013). Global exponential dissipativity and stabilization of memristor-based recurrent neural networks with time-varying delays. Neural Networks, 48, 158-172.

[23] Guo, Z., Wang, J., & Yan, Z. (2015). Global exponential synchronization of two memristor-based recurrent neural networks with time delays via static or dynamic coupling. IEEE Transactions on Systems, Man, and Cybernetics: Systems, 45(2), 235-249.

[24] Abdurahman, A., Jiang, H., & Teng, Z. (2015). Finite-time synchronization for memristor-based neural networks with time-varying delays. Neural Networks, 69, 20-28.

[25] Cai, Z., Huang, L., & Zhang, L. (2016). New conditions on synchronization of memristor-based neural networks via differential inclusions. Neurocomputing, 186, 235-250.

[26] Gao, J., Zhu, P., Alsaedi, A., Alsaadi, F. E., & Hayat, T. (2017). A new switching control for finite-time synchronization of memristor-based recurrent neural networks. Neural Networks, 86, 1-9.

[27] Zhang, W., Li, C., Huang, T., & Huang, J. (2016). Stability and synchronization of memristor-based coupling neural networks with time-varying delays via intermittent control. Neurocomputing, 173, 1066-1072.

[28] Yang, X., Cao, J., & Liang, J. (2017). Exponential synchronization of memristive neural networks with delays: interval matrix method. IEEE Transactions on Neural Networks and Learning Systems, 28(8), 1878-1888.

[29] Chen, J., Zeng, Z., & Jiang, P. (2014). Global Mittag-Leffler stability and synchronization of memristor-based fractional-order neural networks. Neural Networks, 51, 1-8.

[30] Zhang, S., Yu, Y., & Gu, Y. (2017). Global attractivity of memristor-based fractional-order neural networks. Neurocomputing, 227, 64-73.

[31] Wu, A., & Zeng, Z. (2017). Global Mittag-Leffler stabilization of fractional-order memristive neural networks. IEEE Transactions on Neural Networks and Learning Systems, 28(1), 206-217.

[32] Bao, H., Park, J. H., & Cao, J. (2015). Adaptive synchronization of fractional-order memristor-based neural networks with time delay. Nonlinear Dynamics, 82(3), 1343-1354.

[33] Velmurugan, G., Rakkiyappan, R., & Cao, J. (2016). Finite-time synchronization of fractional-order memristor-based neural networks with time delays. Neural Networks, 73, 36-46.

[34] Chen, L., Cao, J., Wu, R., Machado, J. T., Lopes, A. M., & Yang, H. (2017). Stability and synchronization of fractional-order memristive neural networks with multiple delays. Neural Networks, 94, 76-85.

[35] Gu, Y., Yu, Y., & Wang, H. (2016). Synchronization for fractional-order time-delayed memristor-based neural networks with parameter uncertainty. Journal of the Franklin Institute, 353(15), 3657-3684.

[36] Zhang, L., & Yang, Y. (2017). Lag synchronization for fractional-order memristive neural networks via period intermittent control. Nonlinear Dynamics, 89(1), 367-381.

[37] Huang, T., Li, C., Yu, W., & Chen, G. (2009). Synchronization of delayed chaotic systems with parameter mismatches by using intermittent linear state feedback. Nonlinearity, 22(3), 569-584.

[38] Huang, T., Li, C., & Liao, X. (2007). Synchronization of a class of coupled chaotic delayed systems with parameter mismatch. Chaos, 17(3), 033121.

[39] He, W., Qian, F., Lam, J., Chen, G., Han, Q. L., & Kurths, J. (2015). Quasi-synchronization of heterogeneous dynamic networks via distributed impulsive control: Error estimation, optimization and design. Automatica, 62, 249-262.

[40] Huang, X., Fan, Y., Jia, J., Wang, Z., & Li, Y. (2017). Quasi-synchronization of fractional-order memristor-based neural networks with parameter mismatches. IET Control Theory & Applications, 11(14), 2317-2327.

[41] Lu, J. G., & Chen, Y. Q. (2010). Robust stability and stabilization of fractional-order interval systems with the fractional order α: The $0 < \alpha < 1$ case. IEEE Transactions on Automatic Control, 55(1), 152-158.

[42] Sabatier, J., Moze, M., & Farges, C. (2010). LMI stability conditions for fractional order systems. Computers & Mathematics with Applications, 59(5), 1594-1609.

[43] Huang, X., Wang, Z., Li, Y., & Lu, J. (2014). Design of fuzzy state feedback controller for robust stabilization of uncertain fractional-order chaotic systems. Journal of the Franklin Institute, 351(12), 5480-5493.

[44] Ji, Y., Su, L., & Qiu, J. (2016). Design of fuzzy output feedback stabilization for uncertain fractional-order systems. Neurocomputing, 173, 1683-1693.

[45] Hu, J., Wang, Z., Liu, S., & Gao, H. (2016). A variance-constrained approach to recursive state estimation for time-varying complex networks with missing measurements. Automatica, 64, 155-162.

[46] Sheng, L., Zhang, W., & Gao, M. (2014). Relationship between Nash equilibrium strategies and H_2/H_∞ control of stochastic markov jump systems with multiplicative noise. IEEE Transactions on Automatic Control, 59(9), 2592-2597.

[47] Hu, J., Wang, Z., Alsaadi, F. E., & Hayat, T. (2017). Event-based filtering for time-varying nonlinear systems subject to multiple missing measurements with uncertain missing probabilities. Information Fusion, 38, 74-83.

[48] Sheng, L., Wang, Z., Zou, L., & Alsaadi, F. E. (2017). Event-based H_∞ state estimation for time-varying stochastic dynamical networks with state- and disturbance-dependent noises. IEEE Transactions on Neural Networks and Learning Systems, 28(10), 2382-2394.

[49] Hu, J., Wang, Z., Shen, B., & Gao, H. (2013). Quantised recursive filtering for a class of nonlinear systems with multiplicative noises and missing measurements. International Journal of Control, 86(4), 650-663.

[50] Podlubny, I. (1999). Fractional Differential Equations. Acad. Press, London, E2.

[51] Henderson, J., & Ouahab, A. (2009). Fractional functional differential inclusions with finite delay. Nonlinear Analysis, 70(5), 2091-2105.

[52] Filippov, A. F. (1988). Differential Equations with Discontinuous Righthand Sides. Boston, MA: Kluwer Academic Publishers.

[53] Zhang, S., Yu, Y., & Wang, H. (2015). Mittag-Leffler stability of fractional-order Hopfield neural networks. Nonlinear Analysis: Hybrid Systems, 16, 104-121.

[54] Duarte-Mermoud, M. A., Aguila-Camacho, N., Gallegos, J. A., & Castro-Linares, R. (2015). Using general quadratic Lyapunov functions to prove Lyapunov uniform stability for fractional order systems. Communications in Nonlinear Science and Numerical Simulation, 22(1), 650-659.

[55] Cao, J., Ho, D. W., & Huang, X. (2007). LMI-based criteria for global robust stability of bidirectional associative memory networks with time delay. Nonlinear Analysis, 66(7), 1558-1572.

[56] Wang, D., Xiao, A., & Liu, H. (2015). Dissipativity and stability analysis for fractional functional differential equations. Fractional Calculus and Applied Analysis, 18(6), 1399-1422.

[57] Boyd, S., El Ghaoui, L., Feron, E., & Balakrishnan, V. (1994). Linear Matrix Inequalities in System and Control Theory. Philadelphia, PA, USA: SIAM.

[58] Chua, L. O. (2011). Resistance switching memories are memristors. Applied Physics A, 102(4), 765-783.

[59] Clarke, F. H., Ledyaev, Y. S., Stern, R. J., & Wolenski, P. R. (2008). Nonsmooth Analysis and Control Theory. Springer Science & Business Media.

[60] Aubin, J. P., & Cellina, A. (1984). Differential Inclusions: Set-Valued Maps and Viability Theory. Berlin, Germany: Springer.

[61] Shen, J., & Lam, J. (2014). Non-existence of finite-time stable equilibria in fractional-order nonlinear systems. Automatica, 50(2), 547-551.

Yingjie Fan received the B.S. degree from Jinan University, Jinan, China in 2010. He is currently working toward the Ph.D. degree in Control Theory and Control Engineering at the College of Electrical Engineering and Automation, Shandong University of Science and Technology since 2014. His current research interest covers neural networks, memristor-based circuits and systems, and fractional-order nonlinear systems.

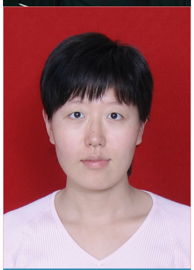

Xia Huang received the M.S. and Ph.D. degree in Applied Mathematics from Southeast University, Nanjing, China in 2004 and 2007 respectively. She has been an Associate Professor at the College of Electrical Engineering and Automation, Shandong University of Science and Technology, Qingdao 266590, China, since 2010. Her current research interest covers neural networks, fractional-order nonlinear systems, memristor-based circuits and systems.

Zhen Wang received the M.S. degree in Computational Mathematics from Ocean University of China, Qingdao, China in 2004. He received the Ph.D. degree in the School of Automation, Nanjing University of Science and Technology in 2014, Nanjing, China. He has been an Associate Professor at the College of Mathematics and Systems Science, Shandong University of Science and Technology, Qingdao 266590, China, since 2015. His current research interest covers fractional-order systems, complex-valued neural networks.

Yuxia Li received the B.Sc degree from Shenyang Jianzhu University, China in 1990, and the Ph.D. degree from Guangdong University of Technology, China in 2005. She has been a Professor at the College of Electrical Engineering and Automation, Shandong University of Science and Technology, Qingdao 266590, China, since 2008. Her current research interest covers memristor-based circuits and systems, nonlinear circuits and systems.